APPLICATION OF ULTRASONIC BEAM MODELING TO PHASED ARRAY TESTING OF COMPLEX GEOMETRY COMPONENTS

O. Roy, S. Mahaut, M. Serre,
Commissariat à l'Energie Atomique,
CEA/CEREM, CE Saclay France

INTRODUCTION

For several years, the French Atomic Energy Commission (CEA) has developed phased array techniques to improve defect characterization and adaptability to various inspection configurations [1]. Such techniques allow to steer and focus the ultrasonic beam radiated by a transducer split into a set of individually addressed elements, using amplitude and delay laws. For most conventional systems, those delay laws are extracted from geometric ultrasonic paths between each element of the array and a geometric focusing point, or experimentally deduced for a detected defect. Geometric delay laws are usually applied to perform beam-forming abilities [2] for simple geometry components (e.g. beam-steering over a plane specimen), whereas experimental delays can be supplied to the array at transmission and reception to optimally adapt the ultrasonic beam to the detected defect, in a so-called self-focusing process [3,4]. This method, relevant for complex material or geometry leading to phase distortion or complex paths that cannot be predicted by simple geometrical calculations, obviously requires the existence of a reflector and the ultrasonic beam radiated by the experimental delay law cannot be known. Therefore this technique is used to improve defect detection (optimal sensibility) rather than defect characterization. To assess complex geometry components inspection with an adaptive system, the CEA has developed new modeling devoted to predict the ultrasonic field radiated by arbitrary transducers through complex geometry and material specimen [5]. A model allows to compute optimized delay laws to preserve the characteristics of the beam through the complex surface, as well as the actual radiated field using those delays. This paper presents two applications of this model : the inspection of a misaligned specimen, and the inspection of an irregular surface.

A COMPUTATION MODEL FOR NDT CONFIGURATIONS : CHAMP-SONS

The Champ-Sons model has been developed for several years [6], and validated using comparisons with other models - angular spectrum and finite elements method [7] - , and experiments [8]. This model, based on the Rayleigh integral extended to take account of refraction through a Fluid/Solid interface, gives accurate and quantitative results assuming that both field computation and source points are not close to the interface (about

Review of Progress in Quantitative Nondestructive Evaluation, Vol. 18
Edited by Thompson and Chimenti, Kluwer Academic/Plenum Publishers, 1999

one wavelength). Contact transducers (with wedge) can also be modeled as shear wave effects can be neglected inside the wedge. The case of directly coupled contact transducers is also currently being implemented.

General Formulation of the Rayleigh Integral

The Rayleigh integral extended to take into account the refraction postulates that the elastic field is the sum of contributions of running source points of the transducer (see Calmon *et al* [6] for a review), which can be expressed as :

$$u(r,t) = \iint_{transd} DF(r_{tr}) C_{\alpha}^{\phi,u}(\theta_f,t) \frac{v_n(r_{tr}, t - t_{shape}(r_{tr}) - T_{path}(r_{tr},r))}{2\pi} dS_{tr} \qquad (1)$$

where $u(r,t)$ is the acoustic quantity considered (e.g. vector displacement, scalar potential), $DF(r_{tr})$ is the divergence factor, $C_{\alpha}^{\phi,u}(\theta_f,t)$ is the transmission coefficient, and $v_n(r_{tr}, t - t_{shape}(r_{tr}) - T_{path}(r_{tr},r))$ is the delayed particle velocity of an elementary source point of the radiating surface Tr.

The divergence factor accounts for the deformation of the wavefront (initially spherical in the coupling medium), ensuring the energy conservation of a ray-pencil propagating along the path of stationary phase. The transmission coefficient, related to the acoustic quantity actually calculated, is a time-dependent coefficient to take account of the possible pulse deformation in the refraction process, as well as converted shear waves. $t_{shape}(r_{tr})$ is related to the geometrical shape of the radiating surface. Multiple diffraction at the surface of the radiating surface may be neglected for smoothly curved radiators [9]. T_{path} is the delay related to the ultrasonic path between the source point and the field computation point, which can be expressed as :

$$T_{path} = \frac{r_f}{c_f} + \frac{r_{\alpha}}{c_{\alpha}} \qquad (2)$$

where r_f (resp. r_{α}) is the wave path in the coupling (resp. specimen) and c_f and c_{α} are the wave speeds in the two media.

Phased Array Features

Various shapes and designs of phased array transducers can be used : annular arrays, linear arrays (1D or 2D). As the transducer radiating surface is modeled as the integrated contribution of point sources, the phased arrays may also be shaped. The ultrasonic field radiated by those array transducers may be expressed as :

$$u(r,t) = \sum_i A_i \iint_{transd_i} DF_i(r_{tr}) C_{\alpha}^{\phi,u}(\theta_f,t) \frac{v_n(r_{tr}, t - t_{shape}(r_{tr}) - T_{path}(r_{tr},r) - \tau_i)}{2\pi} dS_{tr_i} \qquad (3)$$

where A_i and τ_i are, respectively, the delay and amplitude coefficients of the i^{th} element of the array of surface $transd_i$. Those parameters can be calculated by the model from geometric laws, or experimentally measured and supplied to the model.

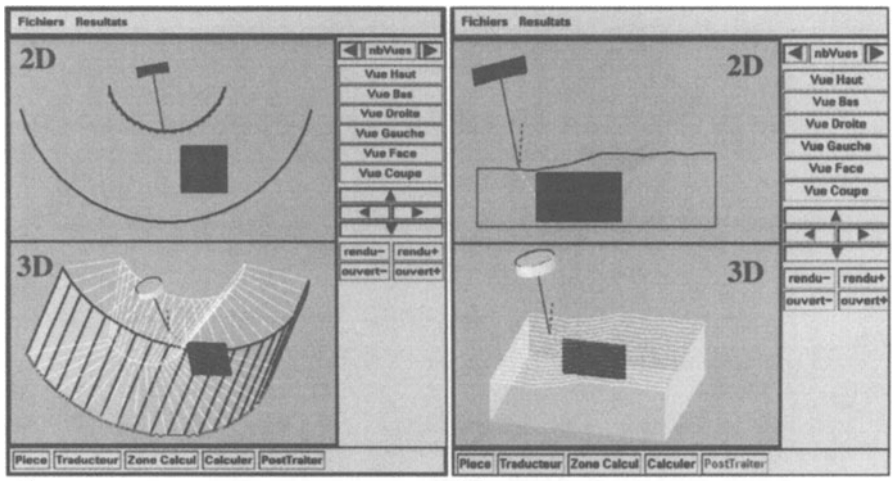

Figure 1. Example of ultrasonic field computation scenes with complex interface geometry, in a) conical specimen inspected from inside, b) CAD surface specimen.

Application to Various Interface Geometry

New developments have been achieved to deal with arbitrary interface shape and materials. Ultrasonic paths between the source point of the transducer and the field computation point can be determined for more complicated specimen, and , moreover, the divergence factor, which accounts for the deformation of the refracted wavefront is itself calculated from the ultrasonic paths and the local derivatives of the interface. This extended model, developed by Gengembre and Lhémery, allows to model any geometry and material (including anisotropic [10] and heterogeneous) specimen.

For single and analytically known interface (planar, cylindrical, conical, spherical, toroidal), the divergence factor can be analytically described [11,12], which is cost-effective for time computing. Computer Aided Design (CAD) surfaces can be used for input data in a user-friendly software, displayed in a whole scene view (display of the whole inspection configuration : transducer, specimen, and computation zone, - profile, 2D or 3D zone -), including rotation and translation of the scene, as illustrated in figure 1.

Application to Beam-Forming Techniques for a Planar Specimen

Figure 2 below shows three different beam-forming techniques performed with a contact array on a steel specimen : focusing, de-focusing and beam-steering. Snapshots of ultrasonic fields, displayed in gray color coding at different transit times, in the computed zone are displayed. The transducer is a 1D linear array of 24 elements of 1.5 mm, operating at 1 MHz (with a 70% bandwidth). The computed area lies on the axis of the array elements, from 2 mm to 42 mm depth , and 60 mm width (30 mm from each side of the transducer axis). In 2.a), the delay law is computed to focus at normal incidence at 20 mm depth, in 2.b), the transducer is arbitrarily unfocused - the delays have been reversed from a) -, while, in c), the delay law is linear in order to get a plane wave at 30° in the specimen. Focusing allows to obtain a high resolution and is required for accurate sizing, whereas an unfocused beam widely insonifies the specimen (for detection with only one single shot), and beam-steering abilities should be performed to assess oriented defects.

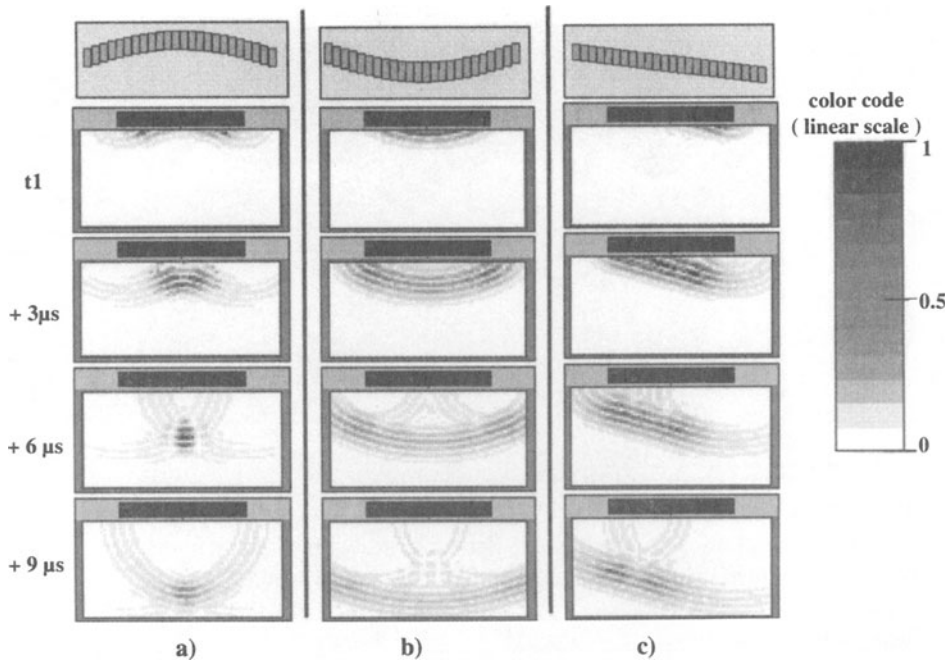

Figure 2. Application of ultrasonic field modeling for a contact array transducer of 24 elements performing : a) depth focusing, b) unfocusing beam, c) beam-steering.

ADAPTIVE INSPECTION OF COMPLEX GEOMETRY SPECIMEN

Inspection of a Misaligned Specimen.

The inspection of misaligned specimen with immersed focused transducers carried out using a conventional scanning system can be drastically degraded. Figure 3 below illustrates the inspection configuration of a misaligned specimen, made of two parts of 25 mm thickness linked through an inclined part, inspected with an immersed focused transducer designed to generate 45° longitudinal waves.

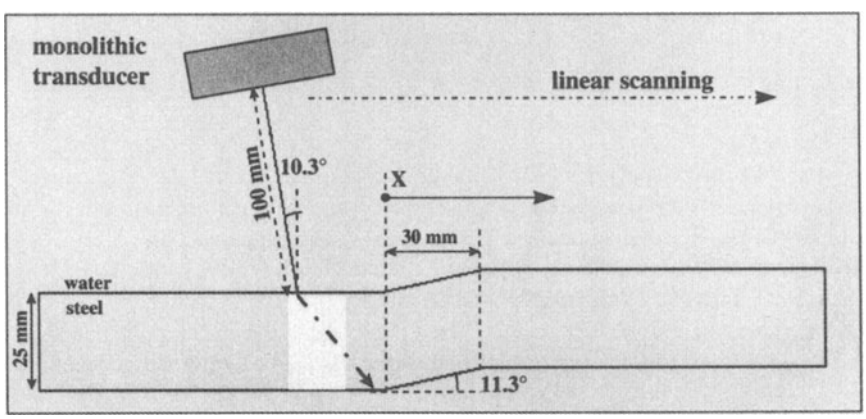

Figure 3. Inspection configuration of a misaligned specimen using a linear scanning system.

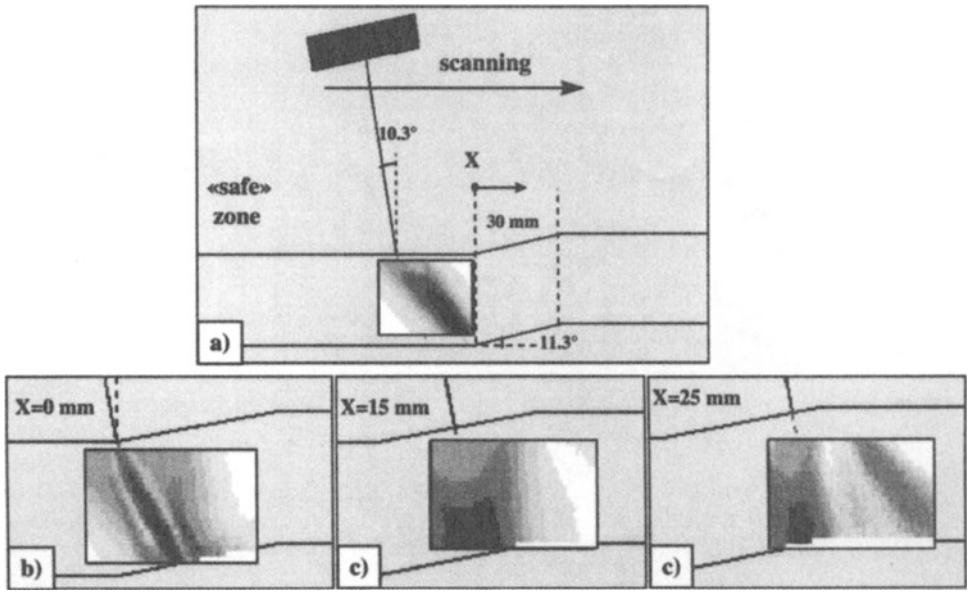

Figure 4. Inspection of a misaligned specimen with a monolithic focused transducer. a) inspection configuration and ultrasonic field transmitted through a « safe » zone, b), c) and d) : ultrasonic fields radiated through different surface misalignments as a function of transducer scanning.

As the transducer moves above the specimen, the refracted beam is degraded The ultrasonic fields (scalar potential) for various scanning positions are displayed in figure 4, in a computed area of 30 mm width * 20 mm height, centered on the desired beam axis of 60° (X is the scanning position, with respect to the projection of transducer axis over the specimen).

- for position X = 0 , waves arising from upper and lower part of the transducer interfere. Contributions of the lower part intersect one of the horizontal parts of the plane specimen, whereas contributions of the upper part intersect an inclined plane, thus generating this cross pattern.
- for position X = 15 (middle of the joining part), the whole beam is deflected by the inclined plane, as the transducer axis is perpendicular to the surface.
- for position X=25 (about the end of the misalignment), the ultrasonic field splits into two beams, which is the reverse effect of position X=0.

As observed in these figures, the ultrasonic beam cannot be preserved through the whole inspection, leading to information loss about the location and sizing of defects. Since the ultrasonic axis is deviated, the position of a defect would be misinterpreted.

To compensate these effects, an adaptive inspection using a phased array and adapted delay laws has been simulated. These simulations have been carried out for each scanning position, delay laws being calculated in order to form the ultrasonic beam in the required area, so as to preserve the ultrasonic beam characteristics (refracted angle, focal depth and beam- width) in spite of the varying surface profile. Delays are calculated from the ultrasonic paths between each element of the array (a 16 element linear array of the same diameter) and a geometric focusing point in the specimen, in order to generate L45° waves and 20 mm depth focusing below the surface.

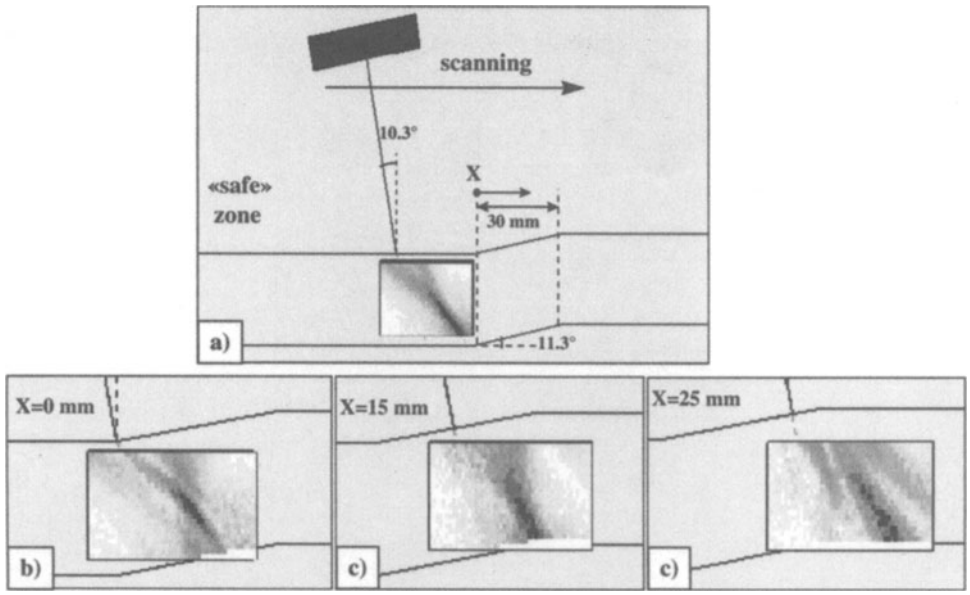

Figure 5. Adaptive inspection of a misaligned specimen with a phased array transducer. a) inspection configuration and ultrasonic field transmitted through a « safe » zone, b), c) and d) : ultrasonic fields radiated at different scanning position, with delay laws supplied to the array.

Ultrasonic fields radiated by the phased arrays are displayed in figure 5. As observed in figure 4, beam distortions are highly reduced by the use of optimized delay laws, even if some lesser geometrical effects still remain. Compared to the monolithic case, it should be pointed out that, for each scanning position, the acoustic energy is centered on the desired beam axis of 60 °, which means that this adaptive inspection would provide quite an accurate defect position, thanks to the preserved beam characteristics.

In addition, it should be noted the acquisition system devoted to perform these techniques allows to adjust all the parameters involved in beam-forming (delays at transmission/reception, and high voltage/amplification, for each acquisition channel), thus the simulation software could also provide a sensibility adjustment profile to be used for each scanning position, combined with adapted delays. Such techniques should provide both constant sizing accuracy and sensibility regardless of the position of the probe.

Adaptive Inspection of a Specimen with an Irregular State of Surface

The last example is related to an irregular surface profile, described as a CAD surface made of arcs and segments, as illustrated in figure 6 below.

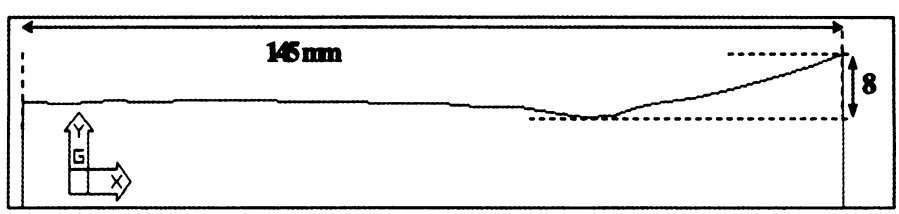

Figure 6. Irregular surface specimen described as a CAD surface.

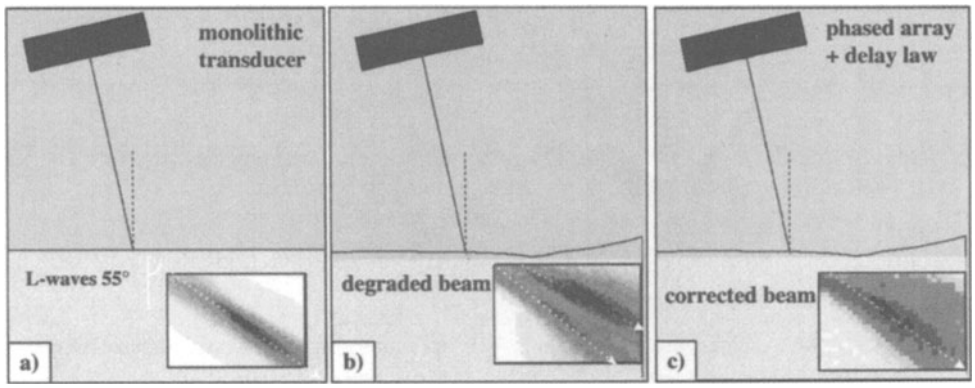

Figure 7. Application of modeling to the adaptive inspection of an irregular surface profile specimen with a monolithic or a phased array transducer. a) regular, planar specimen inspected with a monolithic transducer, b) irregular surface with a monolithic transducer, c) irregular surface with a phased array.

Such irregularities drastically degrades the ultrasonic beam. Display of ultrasonic fields transmitted in the specimen are given in figure 7. Computation areas are 120 mm width and 80mm height, centered on the beam axis.

The ultrasonic field transmitted through a planar, regular profile is displayed in figure 7a) (left), and transmitted through the irregular profile in 7b) (center). Both computed fields are provided using a monolithic focused transducer, with a 50 mm diameter transducer of toroidal surface , operating at 2 MHz, designed to generate 55° longitudinal waves at 40 mm focusing depth. The ultrasonic field transmitted through the irregular surface splits into two beams.

On the same picture, the corrected field radiated by a 24 elements linear transducer is displayed in figure 7c). This simulation has been computed using compensated delays to take account of phased distortion resulting from delayed ultrasonic paths between each element of the array and a geometric focusing point to generate 55° longitudinal waves at 40 mm focusing depth. As observed in the previous example, the ultrasonic field radiated by the phased array supplied with compensated delay laws allows to smear out the distortion effects. However, those effects cannot be fully compensated. Lateral resolution and sensibility cannot be as efficient compared to the planar and regular surface. The ultrasonic beam is larger but it does not split into two beams any more. Therefore, actual measurements should not lead to misinterpretation in this latter adaptive configuration, whereas a single defect would be insonified twice with a classical inspection method.

CONCLUSION

The modeling of phased array techniques has been successfully investigated for two examples typical of complex realistic NDT configurations. The first example is related to the inspection a misaligned specimen, the second one is dedicated to an irregular surface profile. Numerical simulations of ultrasonic fields radiated by monolithic and phased array through complex surface specimen show that the beam distortion can be highly compensated by means of calculated delay laws. The application of such adaptive technique only requires the knowledge of the specimen surface geometry.

These new developments should allow to improve the inspection of complex geometry components considered so far impossible to solve.

REFERENCES

1. S. Mahaut, G. Cattiaux, O. Roy and Ph. Benoist, 14th Int. Conf. on NDE in the Nucl. and Pres. Ves. Ind., 427 (1996).
2. S. Mahaut, O. Roy and M. Serre, Ultrasonics 36, 127 (1998).
3. S. Mahaut, O. Roy, H. Acounis, G. Pincemaille and G. Cattiaux, in *Review of Progress in QNDE*, Vol. 15, eds. D.O. Thompson and D.E. Chimenti (Plenum Press, New-York, 1996), p. 1931.
4. O. Roy, G. Pincemaille, Ph. Morisseau and P. Ancrenaz, 14th Int. Conf. on NDE in the Nucl. and Pres. Ves. Ind., 423 (1996).
5. N. Gengembre and A. Lhémery, in this volume.
6. P. Calmon, A. Lhémery, I. Lecoeur-Taïbi, R. Raillon and L. Paradis, Nuclear Engineering and Design, 180, 271 (1998).
7. P. Calmon, A. Lhémery and J. Nadal, in *Review of Progress in QNDE*, Vol. 15, *op. cit.* (1996), p. 1019.
8. M. El Amrani, P. Calmon, O. Roy, D. Royer and O. Casula, in *Review of Progress in QNDE*, Vol. 14, *op. cit.* (1995), p. 1075.
9. F .Coulouvrat, J. Acoust. Soc. Am, 94, 3 (1993).
10. N. Gengembre, A. Lhémery and P. Calmon, in *Review of Progress in QNDE*, Vol. 17, *op. cit.* (1998), p. 899.
11. A. Lhémery, P. Calmon and M. Méphane, in *Review of Progress in QNDE*, Vol. 16, *op. cit.* (1997), p. 853.
12. S.W. Lee, M.S. Sheshadri M.S. Jamnejad and R. Mittra, IEEE Trans. Microwave Theory Tech., 30, 12 (1982)